Communication

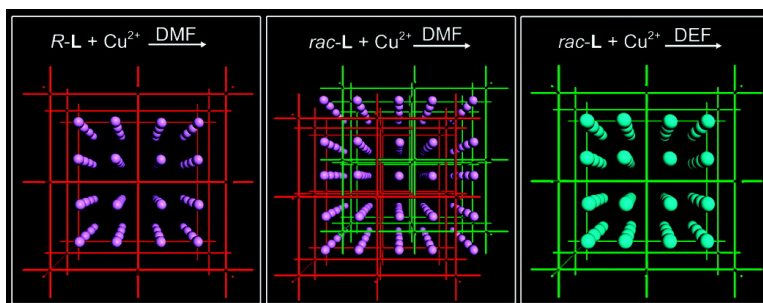# Chirality-Controlled and Solvent-Templated Catenation Isomerism in Metal#Organic Frameworks

Liqing Ma, and Wenbin Lin

More About This Article

Additional resources and features associated with this article are available within the HTML version:

- Supporting Information
- Access to high resolution figures
- Links to articles and content related to this article
- Copyright permission to reproduce figures and/or text from this article

View the Full Text HTML

Chirality-Controlled and Solvent-Templated Catenation Isomerism in Metal−Organic Frameworks

Liqing Ma and Wenbin Lin*

Department of Chemistry, CB#3290, University of North Carolina, Chapel Hill, North Carolina 27599

Received June 27, 2008; E-mail: wlin@unc.edu

Metal organic frameworks (MOFs) have attracted a great deal of recent interest owing to the ability to systematically tune their porosity and the functionalities that are incorporated within the framework scaffolds.[1−3] As a result, numerous MOFs have been engineered for a number of potential applications, including gas storage,[4] nonlinear optics,[2] and catalysis.[5,6] We have particularly demonstrated the utility of binaphthyl-derived homochiral MOFs in heterogeneous asymmetric catalysis.[5a,6] Although a number of strategies have been developed to achieve extremely large porosity in MOFs in recent years,[3] it is still a challenge to obtain MOFs with open channels that are several nanometers in dimensions.[6,7] Such large open channels are essential for asymmetric catalytic reactions because of the need to transport typically very large organic substrates and products.

Increasing the length of bridging ligands can in principle lead to larger channels and pores in the resulting MOFs, but their porosity is often severely reduced as a result of interpenetration of multiple networks (i.e., catenation isomerism). Framework inter-penetration was successfully suppressed in very few MOFs by introducing templating molecules[8] or by reducing reagent concentrations.[9] However, there is no successful example of controlling framework interpenetration in homochiral MOFs.[10] Herein we wish to report an unprecedented catenation isomerism in MOFs that is controlled by both chirality of the bridging ligand and the solvents that were used to grow the MOF crystals.

Blue tetragonal bipyramid crystals (**1**) were obtained from a solvothermal reaction between *R*-**L**-H$_4$ and Cu(NO$_3$)$_2$ in the DEF/H$_2$O mixed solvents at 80 °C (Scheme 1) and had a formula of *R*-[LCu$_2$(H$_2$O)$_2$]·(DEF)$_{12}$·(H$_2$O)$_{16}$ based on single crystal X-ray structure determination and ^{1}H NMR and TGA analyses (Supporting Information). The same reaction carried out in the DMF/H$_2$O mixed solvents led to a polycrystalline product (**2**) that was shown to be isostructural to **1** and to have the formula of *R*-[LCu$_2$(H$_2$O)$_2$]·(DMF)$_{16}$·(H$_2$O)$_{19}$ by powder X-ray diffraction (PXRD) and ^{1}H NMR and TGA analyses.

Single crystal X-ray diffraction studies of **1** revealed a 3-D noninterpenetrating framework crystallizing in the chiral space group *I*4$_1$22 with an asymmetric unit that contains one Cu atom, one half *R*-**L** ligand and one coordinated water for the framework.[11] The Cu atoms coordinate to four carboxylate oxygen atoms of four different *R*-**L** ligands to form [Cu$_2$(O$_2$CR)$_4$] paddle-wheels that are interconnected by the *R*-**L** ligands to form a 3D network (Figure 1a−c). While the carboxylates in the 4,4′-positions reside at either side of the rotational axis of the binaphthyl scaffold, those in the 6,6′-positions are twisted from each other with a dihedral angle of 82.7°. Further examinations revealed that **1** adopts a new (4,4)-connected network topology with the Schlafli symbol {4^3; 6^2; 8}. As a result of the elongated ligand **1**, the noninterpenetrating framework of **1** possesses enormous open channels running through all three directions of the crystals, with the largest openings of 3.2 and 1.5 nm along the *a/b* and *c* axis, respectively (Figure 1d–e).

Scheme 1
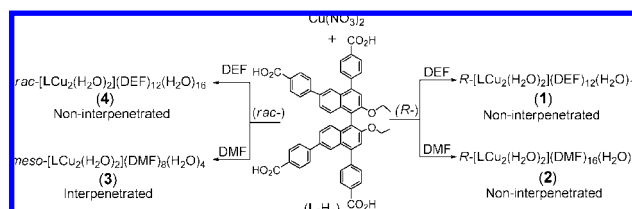
Compound **2** adopts the same framework structure as **1** but contains 16 DMF and 19 water guest molecules instead of 12 DEF and 16 water molecules in **1**. Interestingly, however, when a similar reaction was carried out between *rac*-**L**-H$_4$ and Cu(NO$_3$)$_2$ in the DMF/H$_2$O mixed solvents at 80 °C, a 2-fold interpenetrated 3D MOF (**3**) with the formula of *meso*-[LCu$_2$(H$_2$O)$_2$]·(DMF)$_8$·(H$_2$O)$_4$ was obtained (Scheme 1). **3** has very similar cell parameters as **1** but crystallizes in the centrosymmetric space group *I*4$_1$/*a*.[11] Each of the two interpen-etrating nets in **3** is exactly identical to those of **1** (with the same metal−ligand connectivity and network topology), but they are built from exclusively *R*- or *S*-**L** ligand, respectively. Each crystal of **3** is thus a *meso* compound with two interpenetrating nets of opposite chirality (Figure 2). Owing to the interpenetration of the two enan-tiomeric networks, **3** exhibits much smaller open channels with the largest dimension of ~1.4 nm that are filled with eight DMF and four water molecules. The observation of interpenetration in **3** is remarkable in that the catenation isomerism between **2** and **3** is solely controlled by the chirality of the bridging ligand.

Further analysis of the framework structure of **3** revealed some close contacts between the two interpenetrating nets. The shortest C−C
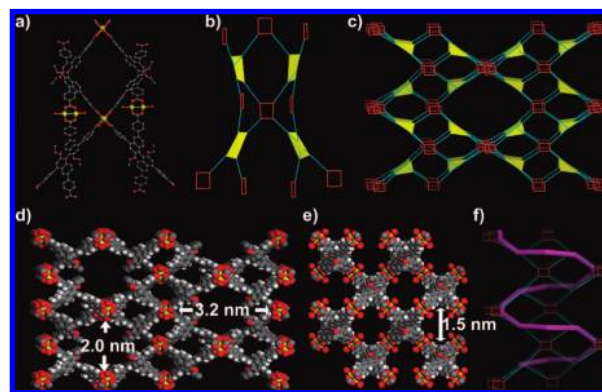

Figure 1. (a) A view of [Cu$_2$(O$_2$CR)$_4$] paddle-wheels and their connectivity with the *R*-**L** ligands in **1**. (b) A simplified connectivity scheme of *R*-**L** ligands (yellow distorted tetrahedra) and [Cu$_2$(O$_2$CR)$_4$] units (red squares). (c) A simplified network connectivity as viewed down the *a* axis. (d) Space-filling model of **1** as viewed down the *b* axis, showing open channels with the largest dimension of 3.2 nm. (e) Space-filling model of **1** as viewed down the *c* axis, showing channels with the largest size of 1.5 nm. (f) The largest channels of 3.2 nm can be described as helices running through both the *a* and *b* axes.
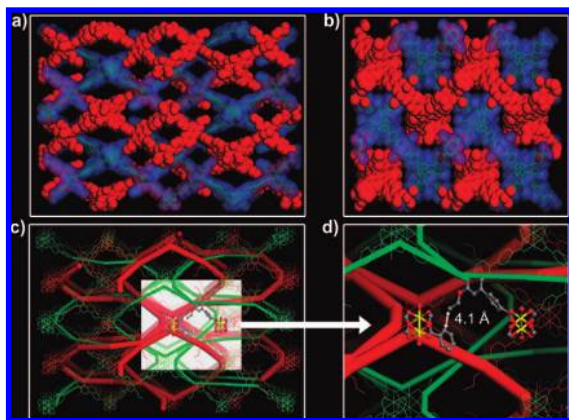
Figure 2. The 2-fold interpenetrating MOF **3**: (a) space-filling model as viewed down the *a* axis (*S* net, blue; *R* net, red); (b) space-filling model as viewed down the *c* axis; (c) interpenetrating networks presented by interwoven arrays of *S*-helix (red) and *R*-helix (green); (d) close contact between *R*- and *S*-nets.

distance between the ethoxyl group and a phenyl ring from the *R* and *S* nets is 4.1 Å (with the corresponding distance between the hydrogen atoms of <3 Å) (Figure 2d). Computer modeling indicated that the shortest C–C distance would have been reduced to ∼1 Å if two homochiral networks were forced to interpenetrate in the same fashion as in **3**, which is physically impossible and explains the unprecedented chirality-controlled catenation isomerism between **2** and **3**.

The remarkable catenation isomerism can also be affected by solvent molecules of different sizes. Reaction of *rac*-**L**-H$_4$ and Cu(NO$_3$)$_2$ in the DEF/H$_2$O mixed solvents at 80 °C led to noninterpenetrating *rac*-[**L**Cu$_2$(H$_2$O)$_2$]·(DEF)$_{12}$·(H$_2$O)$_{16}$ (**4**) that is isostructural to **1** (Scheme 1).[11] Each crystal of **4** is built from the **L** ligands of the same chirality as in **1** but the bulk sample of **4** is racemic. We believe that DMF and DEF molecules act as templates during the crystal growth by coordinating to the Cu centers that are on the surface of a growing single crystal. The larger size of DEF disfavors the formation of interpenetrating MOF owing to the spatial constraints.

Consistent with the very large solvent accessible volume of ∼85% calculated by PLATON[12] for the noninterpenetrating MOFs **1**, **2**, and **4**, they exhibited significant TGA solvent weight loss of 62.0%, 61.8%, and 61.5% in the 25–200 °C temperature range, respectively. In comparison, **3** had a TGA solvent weight loss of 42.8% since the void space constitutes only 70.0% of the crystal.

The permanent porosity of these MOFs was established by nitrogen adsorption at 77 K. After activation at 60 °C under vacuum, the noninterpenetrating MOFs exhibited a BET surface area of ∼240 m^2/g (with pore sizes of 0.8 and 2 nm), whereas the interpenetrating counterpart had a BET surface area of 540 m^2/g (with pore sizes of 0.6 and 1.1 nm) (Figure 3). Although several examples of mesoporous MOFs were recently reported,[7] **1** and **2** represent the first examples of homochiral mesoporous MOFs. The observed surface areas for **1**–**4** are however significantly smaller than the theoretical values (4288 and 2903 m^2/g for **1** and **3**, respectively) obtained from grand canonical Monte Carlo simulations (Supporting Information), suggesting the distortion of the frameworks upon removal of the solvent molecules. Interestingly, **1** readily absorbed 103 wt% of Brilliant Blue R-250 that has a molecular dimension of ∼1.8 nm × 2.2 nm, and the resulting solid exhibited the same PXRD pattern as the pristine **1**. In contrast, **3** absorbed only 10.6 wt% Brilliant Blue because of its smaller channel sizes. These results indicate that the structural integrity and open channels of these mesoporous MOFs are maintained in solution.
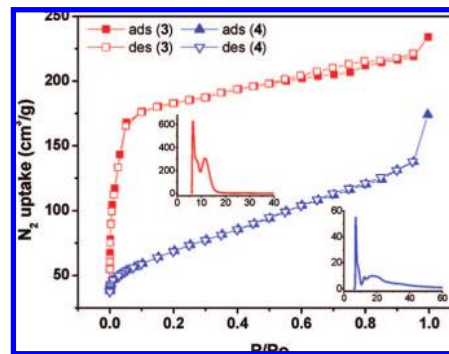

Figure 3. Nitrogen adsorption isotherms of interpenetrating network **3** (red) and noninterpenetrating network **4** (blue). Inset shows their pore size distributions (BJH model) with the *x* axes showing pore diameter in Å and the *y* axes showing Ds(*d*) in m^2/Å/g.

In summary, we have constructed a family of highly porous homochiral, racemic, and meso MOFs based on a new *tetra*-carboxylate ligand and the copper paddle-wheel building units. We have observed remarkable catenation isomerism in this family of MOFs that is controlled by both chirality of the bridging ligand and the size of solvent molecules. The ability to manipulate framework interpenetration is key to future synthesis of mesoporous homochiral MOFs which hold great promise in heterogeneous asymmetric catalysis and chiral separations.

Supporting Information Available: Complete ref 7b; experimental procedures, crystal structure refinement, TGA, XPRD, IR spectra and X-ray crystallographic files. This material is available free of charge via the Internet at http://pubs.acs.org.

References

(1) (a) Moulton, B.; Zaworotko, M. J. *Chem. Rev.* **2001**, *101*, 1629. (b) Yaghi, O. M.; O'Keeffe, M.; Ockwig, N. W.; Chae, H. K.; Eddaoudi, M.; Kim, J. *Nature* **2003**, *423*, 705. (c) Hill, R. J.; Long, D. L.; Champness, N. R.; Hubberstey, P.; Schröder, M. *Acc. Chem. Res.* **2005**, *38*, 335. (d) Bradshaw, D.; Warren, J. E.; Rosseinsky, M. J. *Science* **2007**, *315*, 977.

(2) Evans, O. R.; Lin, W. *Acc. Chem. Res.* **2002**, *35*, 511.

(3) Férey, G.; Mellot-Draznieks, C.; Serre, C.; Millange, F. *Acc. Chem. Res.* **2005**, *38*, 217.

(4) (a) Rosi, N. L.; Eckert, J.; Eddaoudi, M.; Vodak, D. T.; Kim, J.; O'Keeffe, M.; Yaghi, O. M. *Science* **2003**, *300*, 1127. (b) Kesanli, B.; Cui, Y.; Smith, M. R.; Bittner, E. W.; Bockrath, B. C.; Lin, W. *Angew. Chem., Int. Ed.* **2005**, *44*, 72. (c) Chen, B.; Zhao, X.; Putkham, A.; Hong, K.; Lobkovsky, E. B.; Hurtado, E. J.; Fletcher, A. J.; Thomas, K. M. *J. Am. Chem. Soc.* **2008**, *130*, 6411. (d) Pan, L.; Parker, B.; Huang, X.; Olson, D. H.; Lee, J. Y.; Li, J. *J. Am. Chem. Soc.* **2006**, *128*, 4180.

(5) (a) Wu, C.; Lin, W. *Angew. Chem., Int. Ed.* **2007**, *46*, 1075. (b) Dybtsev, D. N.; Nuzhdin, A. L.; Chun, H.; Bryliakov, K. P.; Talsi, E. P.; Fedin, V. P.; Kim, K. *Angew. Chem., Int. Ed.* **2006**, *45*, 916. (c) Cho, S. H.; Ma, B. Q.; Nguyen, S. T.; Hupp, J. T.; Albrecht-Schmitt, T. E. *Chem. Commun.* **2006**, 2563.

(6) Wu, C.; Hu, A.; Zhang, L.; Lin, W. *J. Am. Chem. Soc.* **2005**, *127*, 8940.

(7) (a) Koh, K.; Wong-Foy, A. G.; Matzger, A. J. *Angew. Chem., Int. Ed.* **2008**, *47*, 677. (b) Park, Y. K.; et al. *Angew. Chem., Int. Ed.* **2007**, *46*, 8230. (c) Fang, Q. R.; Zhu, G. S.; Jin, Z.; Ji, Y. Y.; Ye, J. W.; Xue, M.; Yang, H.; Wang, Y.; Qiu, S. L. *Angew. Chem., Int. Ed.* **2007**, *46*, 6638.

(8) (a) Tanaka, D.; Kitagawa, S. *Chem. Mater.* **2008**, *20*, 922. (b) Ma, S. Q.; Sun, D. F.; Ambrogio, M.; Fillinger, J. A.; Parkin, S.; Zhou, H. C. *J. Am. Chem. Soc.* **2007**, *129*, 1858.

(9) Eddaoudi, M.; Kim, J.; Rosi, N.; Vodak, D.; Wachter, J.; O'Keeffe, M.; Yaghi, O. M. *Science* **2002**, *295*, 469.

(10) Garibay, S. J.; Stork, J. R.; Wang, Z. Q.; Cohen, S. M.; Telfer, S. G. *Chem. Commun.* **2007**, 4881.

(11) Crystal data for **1**: tetragonal, *I*4$_1$22, *a* = 24.5377(2), *c* = 72.087(2) Å, *V* = 43404(1) Å^3, ρ_{calcd} = 0.296 g/cm^3. Cell parameter for **3**: tetragonal, *I*4$_1$/a, *a* = 24.5467(12), *c* = 72.387(6) Å, *V* = 43616(5) Å^3, ρ_{calcd} = 0.594 g/cm^3. Cell parameter for **4**: tetragonal, *I*4$_1$22, *a* = 24.5021(5), *c* = 71.809(2) Å, *V* = 43110(2) Å^3, ρ_{calcd} = 0.296 g/cm^3.

(12) Spek, A. L. *J. Appl. Crystallogr.* **2003**, *36*, 7.

JA804944R